Available online at www.sciencedirect.com
SCIENCE DIRECT
ELSEVIER
polymer
Polymer 46 (2005) 10831–10840
www.elsevier.com/locate/polymer

Cure profiles, crosslink density, residual stresses, and adhesion in a model epoxy

Sandra L. Case[a,1], Emmett P. O'Brien[b,2], Thomas C. Ward[a,*]

[a] Department of Chemistry, Virginia Polytechnic Institute and State University, 2107 Hahn Hall, Blacksburg, VA 24061, USA
[b] Department of Chemical Engineering, Virginia Tech, Blacksburg, VA 24061, USA

Received 20 May 2005; received in revised form 8 September 2005; accepted 13 September 2005
Available online 4 October 2005

Abstract

The influence of network chemical composition and cure conditions in a model epoxy system was investigated. Addition of 1,4-butanediol to a bisphenol-F epoxy resin cured with 4-methyl-2-phenyl imidazole led to a decrease in the modulus and glass transition temperature, which resulted in lower residual stresses. Moisture uptake increased with the addition of 1,4-butanediol and is associated with an increase in the free volume of the epoxy. However, even with greater moisture uptake, the addition of 1,4-butanediol to the epoxy increased its adhesion to quartz, primarily through lower residual stress in the samples and increased energy dissipation on debonding. Differences in residual stress for different cure conditions were not measurable in these systems. However, increasing the cure time increased the adhesion of the epoxy to quartz.
© 2005 Elsevier Ltd. All rights reserved.

Keywords: Epoxy; Moisture; Dilatometry

1. Introduction

Residual stresses are introduced in bonded epoxies via cure-induced shrinkage following gelation and also from thermal expansion mismatches between the epoxy and the substrate. The residual stress can be quantified by measuring the curvature of bimaterial specimens, and many investigations have been performed to measure the factors that affect residual stress. Research that varied the cure conditions has shown that increasing the cure temperature increases the residual stress [1–4]. Other studies have indicated that curing epoxies below the glass transition temperature resulted in higher residual stress since, at temperatures less than the glass transition temperature, mobility is reduced and stresses cannot relax [5,6]. Increasing the curing agent concentration, leading to an increase the crosslink density, was also found to increase residual stress [7].

Fluid absorption can also affect residual stress in adhesives by lowering both the glass transition temperature and the modulus, which can lead to stress relaxation in the material. In addition, absorption will generally swell the resin, effectively lowering the tensile stress state that is often present. Voloshin et al. [8] observed that epoxy specimens bonded to silicon relaxed over time at ambient conditions and this was attributed to moisture absorption. Changes in stress relaxation of polyimides have been correlated to the morphology of the polyimide and to the chemical affinity of the polyimide for water [9,10]. Such changes in stress relaxation on penetrant ingression have allowed diffusion coefficients to be determined from changes in curvature of bimaterial specimens [10,11].

In our present work, the network chemical composition of an epoxy and the cure conditions of the epoxy have been varied to quantify their influence on residual stress and adhesion.

2. Experimental

2.1. Materials

A model epoxy system was chosen based on Epon 862®, a bisphenol-F resin (shown in Fig. 1a), obtained from Shell Chemical Corporation. This resin has an epoxide equivalent weight of 171 g/mole. Three parts per hundred resin (phr) of 4-methyl-2-phenylimidazole (Fig. 1b) was used as the curing agent in this model system. In the cure process, the imidazole is added to the epoxy ring to form an imidazole-epoxy adduct. This hydroxy adduct then initiates the epoxy ring opening, leading to chain propagation [12,13]. The concentration of 1,4-butanediol (Fig. 1c) was varied (0, 5, and 10 phr) to examine the effects of

* Corresponding author. Tel.: +1 540 231 5876; fax: +1 540 231 8517.
E-mail address: tward@vt.edu (T.C. Ward).
[1] Present address: Lord Corporation, Cary, NC 27511, USA.
[2] Present address: Eastman Chemical Company, Kingsport, TN 37662, USA.

0032-3861/$ - see front matter © 2005 Elsevier Ltd. All rights reserved.
doi:10.1016/j.polymer.2005.09.053

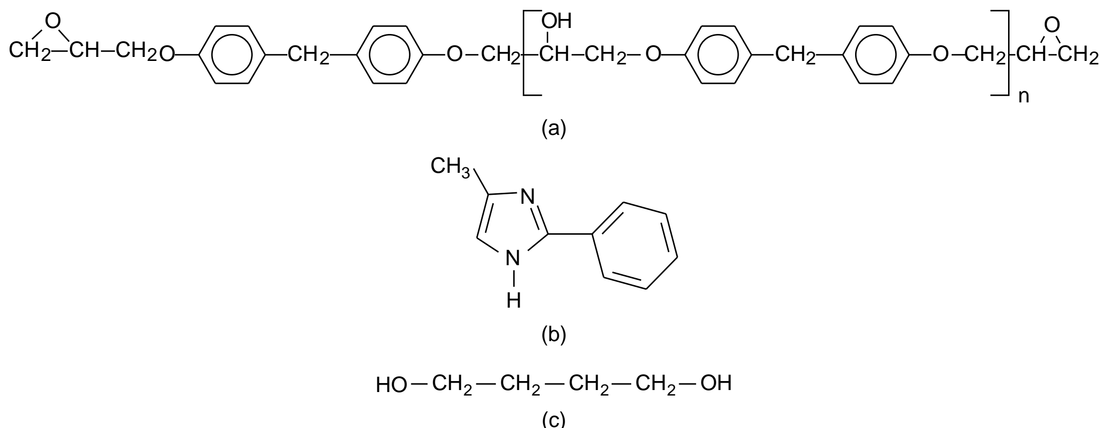

Fig. 1. Model epoxy components. (a) Epon 862® (bisphenol-F epoxy); (b) 4-methyl-2-phenylimidazole; (c) 1,4-butanediol.

network chemical composition on the final epoxy properties. The 1,4-butanediol is thought to toughen the epoxy through chain transfer by either: (1) increasing the number of chain ends if one of the hydroxyl groups reacts, or (2) chain extension when both hydroxyl groups react. Both possibilities lead to a crosslinked network with a lower glass transition temperature. The components of the model epoxy system were thoroughly mixed at 75 °C for 20 min. After casting the adhesive into the test geometry, the specimens were placed in a forced air oven to cure at the desired time and temperature. After the desired cure time was reached, the specimens were removed from the oven and placed on a bench-top to cool to room temperature.

2.2. Dynamic mechanical analysis

The dynamic mechanical properties of the epoxy were obtained using a TA Instruments DMA 2980. The samples were shaped using an aluminum cavity mold yielding the specimen geometry of approximately $52\times5\times2\ mm^3$. Samples were sanded to obtain uniform thicknesses of ±0.02 mm. Measurements were taken in the dual cantilever mode using a frequency of 1 Hz. An oscillation amplitude of 20 μm was employed at a heating rate of 3 °C/min. Three samples of each type were measured. The average and one standard deviation of the modulus are reported.

2.3. Density

Rectangular samples of the cured epoxy were sanded to uniform dimensions with thickness and width variations of ±0.03 mm and ±0.01 mm, respectively. The dimensions were measured with a micrometer having a 0.01 mm resolution. The sample length was fixed at 52 mm. The mass was measured using a Mettler AE200 analytical balance with a 10^{-4} g resolution. The average and one standard deviation of the density are reported.

2.4. Tensile modulus

An aluminum mold was fabricated in accordance with ASTM D 638 IV to prepare epoxy dogbone test specimens. The samples were 1.5 mm thick with a gauge length of 25.4 mm. Samples were measured using an Instron, model 1321, with a 1 kN load cell at a crosshead displacement of 13 N/s. The strain was measured using a Fiedler Optoelktronik Laser Extensometer, model P-2A-50. The average and one standard deviation of the modulus are reported.

2.5. Residual stress

To determine the influence of cure profiles and the 1,4-butanediol content on residual stress, the liquid epoxy mix was coated onto and subsequently cured on borosilicate glass slides. These Gold Seal® borosilicate glass cover slides ($65\times48\times0.15\ mm^3$) were obtained from VWR Scientific Products. The glass slides were cleaned in a 1:1:5 (v/v/v) boiling solution of hydrogen peroxide (30%), ammonium hydroxide, and water for 1 h. The glass was cut into strips (48×8 mm) after cleaning, and then coated with the epoxy ($\sim$300 μm thick) using a pneumatically driven doctor blade. In order to prevent recontamination, the glass slides were coated with the adhesive within 24 h of cleaning. The coated strips were placed on a piece of aluminum, 6.35 mm thick and placed in an oven at preset conditions for cure. Samples were covered during this cure with a Petri dish cover to isolate them from the forced air being circulated in the oven to prevent dewetting along the specimen edges.

The formation of residual stresses arising from the curing and cooling of the epoxy bonded on the glass was detected by sample curvature in the composite structure. Measuring this amount of curvature allows a calculation of the responsible residual stress [14,15]. The radius of curvature of the composite specimen was obtained using a TA Instruments DMA 2980 using a modification of a technique developed by Dillard et al. [16,17]. Measurements were taken on borosilicate glass strips ($48\times8\times0.15$ mm) coated with the model epoxy (0.3 mm thick). The deflection of the curved samples was measured with a modified penetration clamp geometry, shown in Fig. 2. A top crossbar was fabricated to hold a probe that could be used to measure sample position. A 3.175 mm diameter steel ball bearing was used for the probe tip. The DMA was operated in the penetration clamp geometry and in

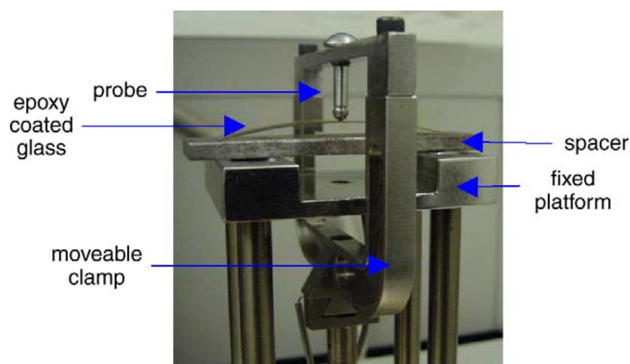

Fig. 2. DMA curvature measurement setup. The probe is resting on a curved piece of glass coated with the epoxy.

the controlled force mode. The sample was placed on a flat surface after the position of the DMA probe resting on this surface had been recorded as zero. A force of 0.010 N was applied in order to maintain 'light' contact with the sample and the position of the DMA probe resting on the sample was recorded. Samples were examined with the glass-side up. The average and one standard deviation of the measured deflection and calculated residual stress are reported.

2.6. X-ray photoelectron spectroscopy

A PHI Perkin Elmer model 5400 X-ray photoelectron spectrometer (XPS) was used to examine the borosilicate glass prior to and after cleaning. Analysis was carried out using Mg K_α X-rays ($h\nu=1253.6$ eV) at 300 W and 14 kV. Ejected electrons were detected using a hemispherical analyzer. A 1×3 mm spot size was analyzed using a 45° take off angle. The sampling depth is approximately 50 Å.

2.7. Dilatometry

Length changes of the epoxy as a function of temperature were measured using a Netzsch Dilatometer 402C. A 0.30 N force, insufficient to cause detectable penetration at the temperatures examined, was applied, and the epoxy samples were heated at 2 °C/min. under a nitrogen purge. The samples were cast in aluminum molds and were approximately 5 mm wide and 2 mm thick. The sample length varied between 15 and 18 mm. The average and one standard deviation of the coefficient of thermal expansion are reported.

2.8. Adhesion—shaft loaded blister test

The adhesion of the model epoxy coated on the quartz was measured using a shaft loaded blister test. This experiment uses the controlled displacement of a spherically capped shaft driven by a universal testing machine to create a growing blister as an alternative to applying fluid or gas media to generate the fracture [18–25]. Quartz substrates, 38 mm$\times$38 mm$\times$6 mm, with an 8 mm diameter hole in the center were used. The quartz substrates were cleaned by boiling them in 18 M sulfuric acid for 1 h. This cleaning method provided a way to entirely remove the cured epoxy from previous experiments enabling the quartz specimens to be reused. A circular piece of Kapton® backed acrylic PSA tape (obtained from McMaster Carr), 12.7 mm diameter, was used to cover the hole on one side of the quartz and also served as the pre-crack. Our model epoxy (0.15 mL) was dispensed on the quartz substrate on the face with the Kapton® PSA tape. Squares of Kapton® E film (0.05 mm thick) were cut slightly larger than the quartz substrate and applied on top of the model epoxy to provide a mechanical reinforcing layer to prevent the shaft from puncturing through the epoxy. These specimens were placed in the oven at a designated cure temperature and time. After curing, the samples had an epoxy thickness of approximately 50 μm.

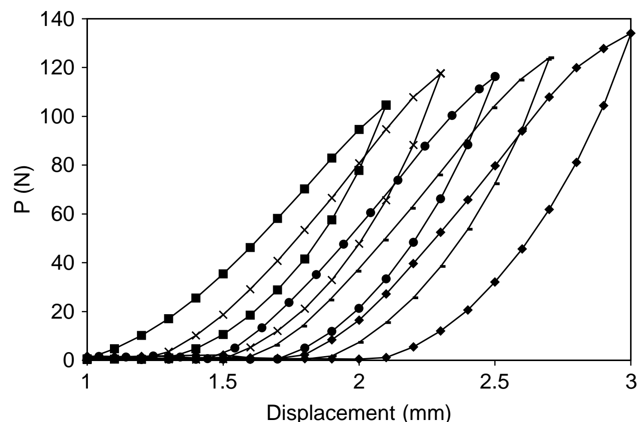

Fig. 3. SLBT load versus displacement.

The specimens were placed in various environments for conditioning prior to testing. Samples were conditioned at room temperature in 70% relative humidity for 36 h, or in water at room temperature for 36 h, or in water at 60 °C for 24 h.

Debonding energies were evaluated for the model epoxy bonded to quartz specimens using an Instron, model 5500R. A shaft with a 0.64 mm diameter ball bearing was attached to a 25 kN load cell and aligned with the blister hole. The shaft was driven at 6 mm/min to a preset displacement and then unloaded. The load at the maximum displacement was recorded. The sample was then removed from the testing apparatus, and the diameter of the resulting debond was measured in two perpendicular in-plane directions. The sample was then placed back in the testing apparatus and loaded to a greater displacement. This procedure was repeated until the crack diameter reached the size of the quartz substrate. An example of a typical load versus displacement result is shown in Fig. 3.

3. Results and discussion

3.1. Dynamic mechanical analysis—butanediol content

Dynamic mechanical analysis (DMA) was used to examine the viscoelastic properties of the model epoxy having differing concentrations of 1,4-butanediol cured at 130 °C for 1 h.

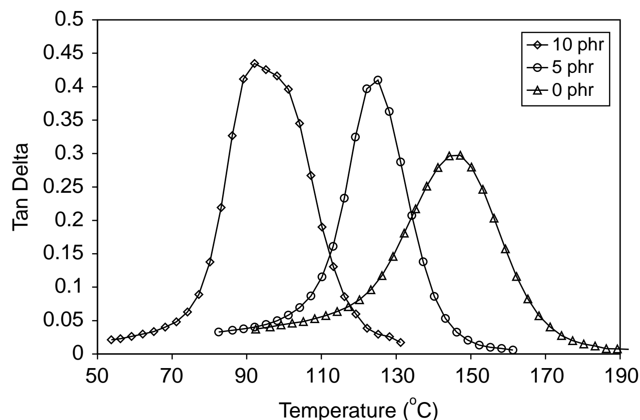

Fig. 4. Tan Delta: model epoxy with varying 1,4-butanediol content.

This reaction condition produced essentially complete cure of the epoxy, as indicated by a negligible DSC residual exotherm obtained on the final product. Tan delta and modulus as a function of temperature are shown in Fig. 4 and Fig. 5, respectively. From the tan delta peak values, it can be seen that the glass transition temperature decreases substantially with increasing 1,4-butanediol content up to 10 phr. The amplitude and area of the tan delta curve, related to energy dissipation of the sample, also increased with the addition of 1,4-butanediol. From Fig. 5 it is also apparent that the rubbery modulus decreases as the of 1,4-butanediol content was increased. Both the room temperature and rubbery moduli obtained from DMA are reported in Table 1. From rubber elasticity theory, the rubbery modulus is proportional to the crosslink density [26]. Thus increasing the 1,4-butanediol content is concluded to lower the crosslink density of the sample and lead to a decrease in the specific gravity of the sample. This is confirmed by examination of Table 2 which shows the density decreasing with increasing amounts of 1,4-butanediol as a result of increased free volume.

The DMA storage modulus, E', measured at room temperature for samples cured at 130 °C for 1 h (Table 1), shows a linear decrease with the addition of 1,4-butanediol. However, the absolute value (∼7000 MPa) is larger than would be expected for a glassy epoxy. The modulus at room temperature was, therefore, more accurately obtained using a

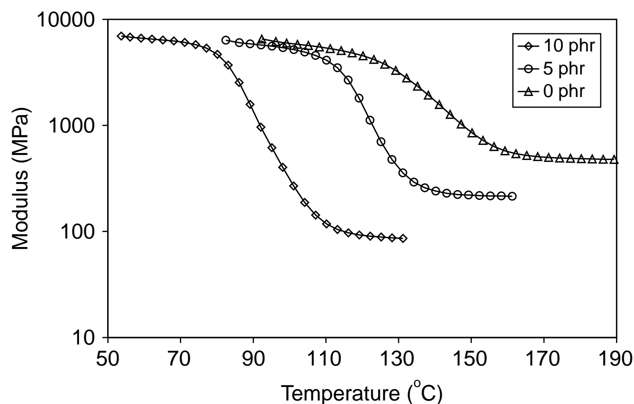

Fig. 5. DMA modulus: model epoxy with varying 1,4-butanediol content.

Table 1
Epoxy modulus values as a function of 1,4-butanediol content

Sample (phr 1,4-butanediol)	DMA modulus, E', (RT) (MPa)	DMA modulus, E', (rubbery) (MPa)	Tensile modulus (RT) (MPa)
0	7879±172	486±57	2907±74
5	7034±388	220±10	2629±107
10	6522±576	92±17	2727±155

tensile dogbone test, and the values are also shown in Table 1. These modulus values are approximately 2700 MPa which is closer to the expected results for a glassy network. However, within the error of the experiment, no substantial differences were observed in the modulus of the various sample compositions using this technique.

3.2. Residual stress

The residual stress of the model epoxy coated on borosilicate glass was calculated using [14,15]

$$\sigma_r = \frac{1}{\rho}\left(\frac{1}{ht_p}\left[\frac{E_p t_p^3}{6} + \frac{E_s t_s^3}{6}\right] + \frac{t_p E_p}{2}\right) \quad (1)$$

where t_p and t_s are the thickness of the polymer and substrate, respectively, E_p and E_s are the moduli of the polymer and substrate, respectively, and h is the total thickness (t_p+t_s). The values for E_p were taken from the tensile experiment, as reported in Table 1, and an accepted value for quartz of 7×10^{10} Pa was chosen for E_s. The radius of curvature, ρ, was determined from the deflection, δ, measured in the DMA as follows [14]

$$\rho = \frac{l^2}{8\delta} \quad (2)$$

where l is the length of the specimen.

3.2.1. Glass cleaning, chemical analysis, and coating

It was necessary to clean the borosilicate glass before coating with the epoxy. XPS results of the uncleaned and cleaned borosilicate glass are shown in Fig. 6 and Table 3. The most significant difference associated with cleaning is in the surface carbon content; prior to cleaning the glass has a carbon concentration of 41%, and after cleaning, the carbon content drops to 13%. Thus, cleaning the glass removes hydrocarbons and makes the surface more readily wettable by the epoxy. The XPS evaluated compositions of the other elements on the surface are also seen to increase following cleaning, reflecting the removal of the hydrocarbon layer. The results, in Table 3, were compared to those for a sample that had only been etched

Table 2
Density as a function of 1,4-butanediol content

Sample (phr 1,4-butanediol)	Density (g/cm³)
0	1.19±0.033
5	1.17±0.008
10	1.15±0.015

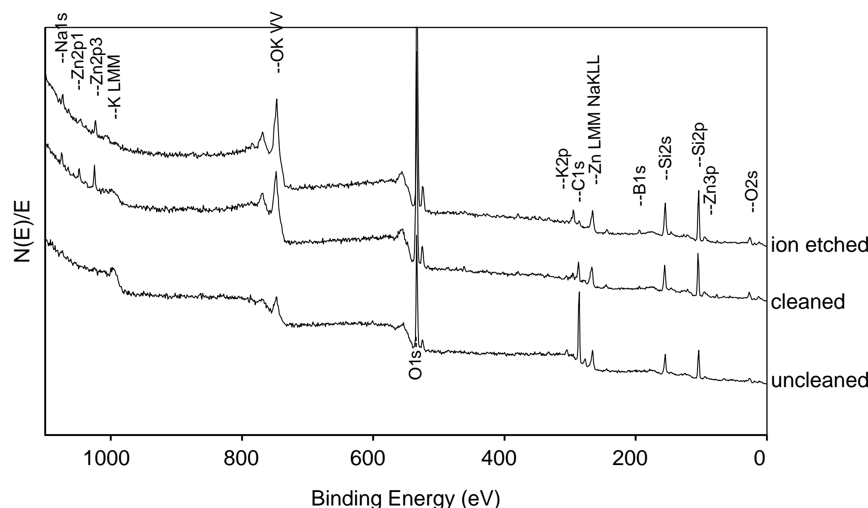

Fig. 6. XPS widescans of cleaned, uncleaned, and ion etched borosilicate glass.

in the XPS with a three keV Argon ion beam for 3 min prior to analysis. This ion-etch was used to remove surface layers at approximately 5 Å/min in order to verify that the observed elements were present in the glass and not a result of introducing contaminants during the cleaning process. The results for the chemically cleaned surface and ion etched surface are very similar indicating that chemically cleaning the surface did not introduce contaminants.

3.2.2. Butanediol content

The effect of the 1,4-butanediol content (0, 5, and 10 phr) on residual stresses in the model epoxy was also examined. For these measurements, all samples were 'fully' cured at 130 °C for 1 h. Table 4 shows the results of the observed residual stress as a function of 1,4-butanediol content. The values represent the average of at least ten samples, and the error bars represent one standard deviation. The addition of the 1,4-butanediol is seen to lead to a linear decrease in the calculated residual stress. Residual stresses can be estimated using [16]:

$$\sigma_r = -\alpha E(\Delta T) \quad (3)$$

where α is the coefficient of thermal expansion, E is the Young's modulus of the material, and ΔT is the change in temperature between the measurement temperature and the stress free temperature. In our samples, the decrease in residual stress with increasing butanediol content is most probably due to the lowering of the crosslink density (increased free volume) with the addition of the 1,4-butanediol, which lowers the modulus and stress-free temperature and accelerates relaxation processes.

To find the stress free temperature (SFT) of the samples, the deflection of the borosilicate glass strips coated with the model epoxies was measured as a function of temperature in the DMA. The results are plotted in Fig. 7. The SFT was determined from the extrapolated slope intersection with a zero deflection line as indicated by the 10 phr sample in Fig. 7. The values of the SFT for the average of three samples are reported in Table 5. As expected, increasing the 1,4-butanediol content, which lowered the glass transition temperature, also lowered the SFT. This conclusion is consistent with all the above trends which also lead to the observed reductions in residual stress.

The relationship of SFT to the T_g and the cure temperature in these results is consistent with the work of Bair et al. [27], who determined that the SFT is approximately equal to the cure temperature when the $T_g > T_{cure}$. In our results, using the tan delta peak as the T_g, for the samples with no butanediol, the T_g was greater than the T_{cure} by approximately 20 °C, and the SFT is approximately equal to the T_{cure}. For the samples with 10 phr butanediol, the T_g is less than T_{cure} by approximately 40 °C and the SFT is approximately equal to the T_g. For samples with 5 phr butanediol, the T_{cure} was approximately *equal* to T_g, and the SFT, T_g and T_{cure} are approximately equal. Thus our

Table 3
XPS analysis of cleaned and uncleaned borosilicate glass

Element	% Atomic concentration uncleaned surface	% Atomic concentration cleaned surface	% Atomic concentration ion etched
C	41.4	13.3	4.2
O	35.4	57.2	61.3
Si	19.5	21.4	24.9
Na	0.6	1.7	1.3
K	0.9	0.9	1.9
B	1.7	2.1	4.0
Al	0.6	2.0	1.0
Zn	nd	0.9	0.4
Ti	nd	0.6	0.8

nd, not detected (less than 0.2%).

Table 4
Deflection and residual stress for the model epoxy coated on borosilicate glass

Sample (phr 1,4-butanediol)	δ (mm)	σ_r (MPa)
0	2.60±0.25	7.19±0.73
5	2.34±0.14	6.48±0.43
10	1.99±0.23	5.49±0.64

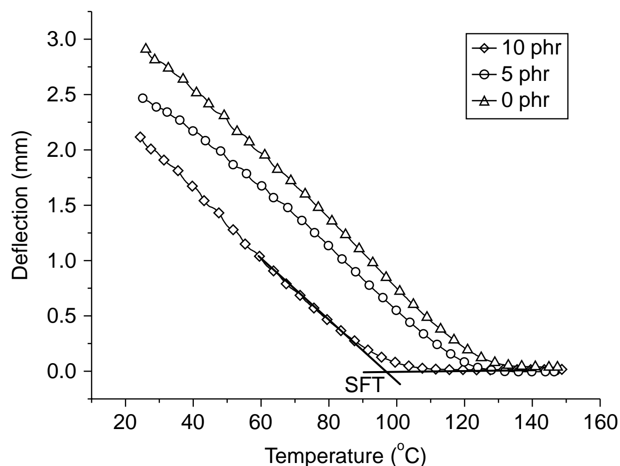

Fig. 7. Deflection versus temperature: model epoxy with varying 1,4-butanediol content.

observations agree with and extend the conclusions about SFT and cure temperature.

3.3. Dilatometry—butanediol content

The impact of changing concentrations of 1,4-butanediol on the model epoxy cured at 130 °C for 1 h was investigated via dilatometry, and the results are shown in Fig. 8. Unlike the typical dilatometric response for amorphous polymers, these model epoxy samples initially shrink as they pass through their glass transition temperatures. It is important to note that upon a second heating cycle, as shown in Fig. 9, the traditional behavior is observed. This eliminates the possibility that the shrinkage is due to sample penetration by the instrument probe. On heating the samples in the dilatometer, the polymer chains acquire mobility on the experimental time scale in the vicinity of the glass transition temperature. As the polymer chains relax, stresses that were created during cure are released [28]. This leads to the observed shrinkage detected for these epoxy samples. The networks containing 10 phr 1,4-butanediol exhibit the greatest shrinkage. This was unexpected since these samples exhibited the lowest measured residual stress, and it was expected that the magnitude of shrinkage observed in the dilatometer would correlate with the residual stress. However, as previously discussed, these samples have the lowest crosslink density and therefore have the greatest amount of free volume. The resulting lower T_g and the promotion of cooperative motions created by free volume are capable of relieving more residual stresses, allowing macroscopic shrinkage in a subsequent reheating, and, hence, they exhibit the greatest shrinkage in the dilatometer.

Table 5
Stress free temperature for the model epoxy coated on borosilicate glass

Sample (phr 1,4-butanediol)	SFT (°C)
0	122.6 ± 0.6
5	117.7 ± 0.9
10	97.8 ± 4.3

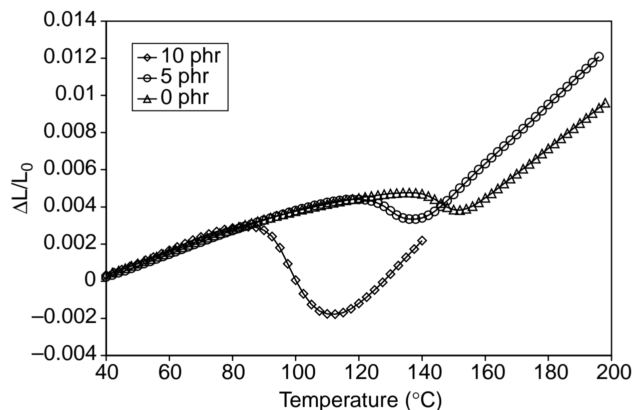

Fig. 8. Dilatometry results as a function of 1,4-butanediol content in the model epoxy.

Increasing the 1,4-butanediol content also increases the CTE in both the glassy and rubbery region, as shown in Table 6. Logically, an increase in free volume at any temperature generates more fluctuations in molecular structure and thus leads to an increase in the rate of expansion upon heating.

3.4. Moisture uptake and stress relaxation—butanediol content

Moisture absorption at 60 °C in unbonded epoxy samples cured at 130 °C for 1 h was also measured for the different 1,4-butanediol content specimens and is shown in Fig. 10. Clearly, changes in free volume, discussed previously, lead to changes in moisture uptake properties. First, increasing the 1,4-butanediol content, which subsequently increases the free volume, led to an increase in the moisture saturation concentration in the epoxy. Saturation mass increases (%) are reported in Table 7. Second, the diffusion coefficient (D) was calculated from a plot of weight percent versus square root of time from the following equation [29]:

$$D = \pi\left(\frac{sb}{4M_\infty}\right)^2 \tag{4}$$

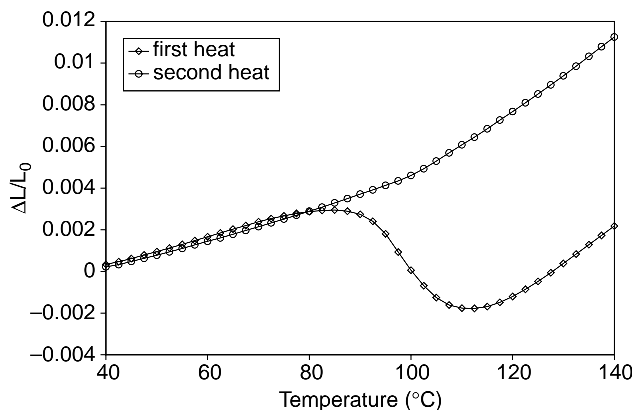

Fig. 9. Dilatometry results for a sample with 10 phr butanediol cured at 130 °C for 1 h, first and second heats.

Table 6
CTEs of the model epoxy as a function of 1,4-butanediol content

Sample (phr 1,4-butanediol)	Glassy CTE (ppm/°C)	Rubbery CTE (ppm/°C)
0	48.9±6.2	135.5±1.7
5	58.9±5.3	160.3±2.4
10	69.4±2.4	177.5±8.5

Table 7
60 °C moisture uptake in the model epoxy

Sample (phr 1,4-butanediol)	M_∞ (%)	D (cm^2/s)
0	1.33±0.07	$1.44\pm0.17\times10^{-8}$
5	1.65±0.10	$1.38\pm0.16\times10^{-8}$
10	2.47±0.10	$1.34\pm0.21\times10^{-8}$

where s is the slope of the initial linear portion of the plot, M_∞ is the percentage of moisture at equilibrium content, and b is the sample thickness. For each 1,4-butanediol level, the diffusion coefficients are listed in Table 7. Within the experimental error, no differences were observed in these diffusion coefficients even though the curves in Fig. 10 look different. This indicates that initially the rate of sorption is the same even though the equilibrium saturation percentages differ.

After saturating dogbone samples, containing 10 phr of 1,4-butanediol cured at 130 °C for 1 h, in water at 60 °C, their tensile response was evaluated. Absorption of moisture leads to a decrease in the modulus from 2727±155 to 2243±91 MPa. It is also well known that even slight water absorption leads to substantial decreases in the glass transition temperature of epoxies. Decreasing the glass transition temperature and decreasing the modulus both contribute to stress relaxation.

It was of interest to determine how exposure to water would influence the residual stress in these epoxies. The curvature of the bimaterial composites consisting of epoxy coated on borosilicate glass was also measured as a function of moisture ingression over time at 60 °C and is shown in Fig. 11. As the water diffuses into the epoxy, contributions from swelling and stress relaxation produce a decrease in the deflection of the sample. (The residual stress, therefore, also decreases; however, value was not calculated since this would require knowledge of the swollen samples' moduli at each water content.)

3.5. Adhesion—butanediol content

Fig. 12 displays the SLBT adhesion results for the model epoxy, cured at 130 °C for 1 h, based on different amounts of 1,4-butanediol. All specimens were conditioned at 70% relative humidity at room temperature for 3 days. All the data for three samples at each concentration of 1,4-butanediol are shown. Best-fit lines were fitted through the data points. Analysis of the experiments reveals that a significantly higher load (approximately 100 N) is required for crack propagation in the sample with 10 phr 1,4-butanediol when compared to the samples having either 0 or 5 phr 1,4-butanediol (approximately 30 N). Within the experimental error, no difference was found between adhesion results for the 0 and 5 phr samples. Fig. 13 illustrates the fracture debonding behavior of the samples. At 10 phr, the crack growth occurs in a symmetric fashion suggesting that the crack driving stress is more evenly distributed around the emerging crack tip. In contrast, for the epoxy having 0 phr, the sample displays a more irregular pattern and appears to fracture in a more brittle manner with random crack growth geometry.

More aggressive environments produced lower failure forces. Specifically, fracture data for samples soaked in water at room temperature for 3 days are shown in Fig. 14. The adhesion is clearly lower than the previously discussed 70% relative humidity samples for each type of epoxy, and again, the 10 phr sample exhibits the highest adhesion according to the shaft loaded blister test. Also shown in this plot are the results for samples conditioned at 60 °C for 24 h prior to testing. The adhesion is reduced dramatically in this most hostile environment and no difference was distinguished for the different sample chemistries.

The 70% relative humidity and room temperature water soaked sample containing 10 phr of 1,4-butanediol has the best adhesion to quartz in a variety of water contents. Recall that the addition of 1,4-butanediol leads to an increase in the amplitude

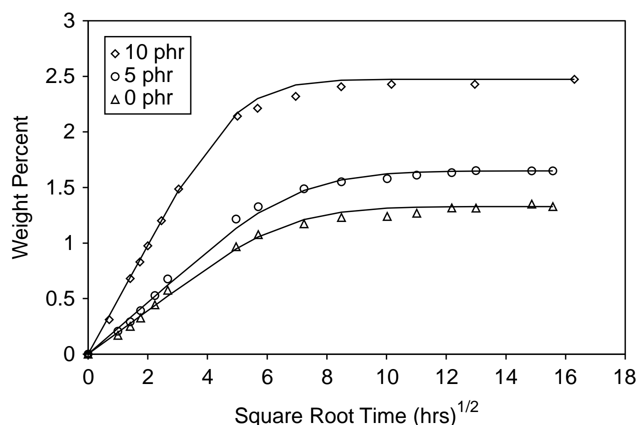

Fig. 10. Moisture uptake results at 60 °C as a function of 1,4-butanediol content in the model epoxy.

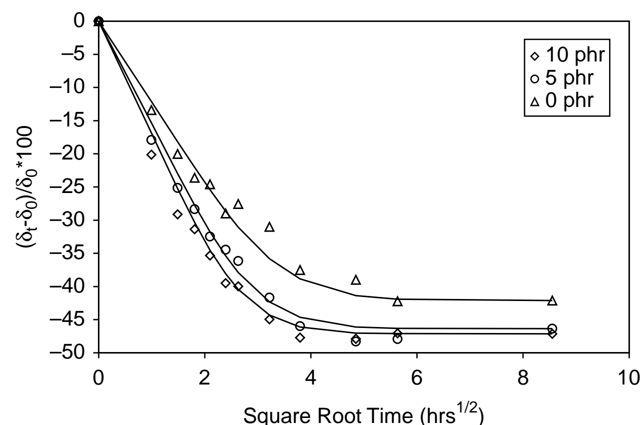

Fig. 11. About 60 °C water-induced relaxation of bimaterial specimens of the model epoxy with differing 1,4-butanediol contents coated on quartz.

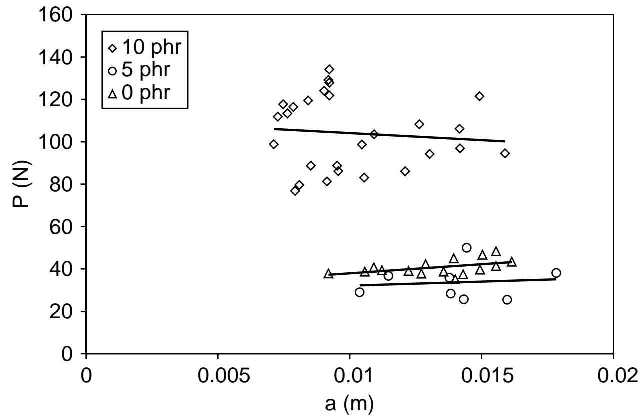

Fig. 12. SLBT loads and displacements (P and a) for epoxies with various 1,4-butanediol content. Samples were conditioned at 70% relative humidity at room temperature for 3 days.

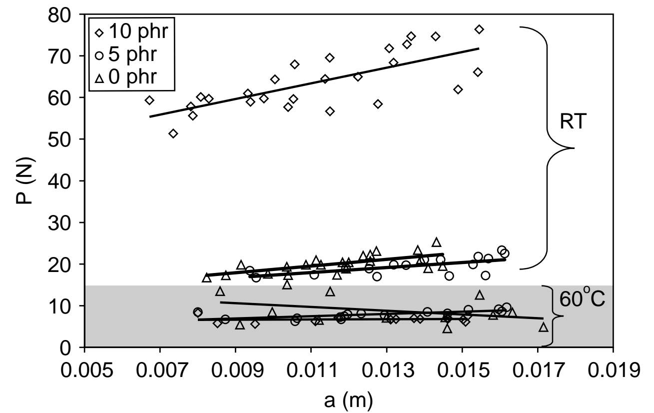

Fig. 14. SLBT loads and displacements (P and a) for three model epoxies having indicated 1,4-butanediol contents. The samples were given a water soak for either 3 days at room temperature or 1 day at 60 °C. (Note: RT, room temperature)

of tan delta, indicating the capability of such materials to dissipate more energy under the right conditions. The 1,4-butanediol also lowers the glass transition temperature, which leads to a reduction of residual stress. These factors aid in increasing the adhesive strength, even though the samples simultaneously exhibit greater moisture uptake.

3.6. Cure conditions

The influence of different time/temperature cure profiles for our model epoxy with 10 phr 1,4-butanediol was also determined. This epoxy with 10 phr 1,4-butanediol was reacted at various conditions and dilatometric response was obtained for:

- 130 °C, 1 h cure
- 80 °C, 2 h cure, with a 180 °C, 2 h postcure
- 130 °C, 1 h cure, with a 180 °C, 2 h postcure.

The results are presented in Fig. 15, from which we note that all of these samples shrink as the epoxy passes through the glass transition range. Curing more slowly (80 °C, 2 h/180 °C, 2 h) produced less shrinkage as observed in the dilatometer than curing more rapidly (130 °C, 1 h). In order to ensure that the primary factor in this outcome was the slower initial cure step, additional samples were cured at 130 °C for 1 h followed by the same 180 °C postcure for 2 h. Within the experimental error, the results observed for this new sample were identical to samples having a 130 °C, 1 h cure with no postcure step. Thus, curing at lower initial temperatures for longer times generates less stress in the resulting epoxy—this translates to less shrinkage in the dilatometer when the sample is reheated.

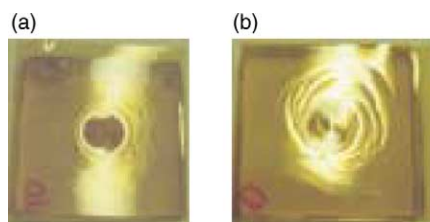

Fig. 13. SLBT crack growth behavior—(a) 10 phr 1,4-butanediol, (b) no 1,4-butanediol.

The water gain on soaking at 60 °C was measured for two of the cure conditions for the sample with 10 phr 1,4-butanediol, and the results are shown in Fig. 16. The saturation mass increases were 2.27±0.09% and 2.47±0.10% for the 80 °C (2 h)/180 °C (2 h) cure and 130 °C (1 h) cure, respectively. The densities of these samples were also measured and found to be 1.16±0.002 g/cm^3 and 1.15±0.015 g/cm^3 for the 80 °C (2 h) /180 °C (2 h) cure and for the 130 °C (1 h) cure, respectively. Although the values determined for the density and the moisture uptake overlap within the error of the experiments for the different cure conditions, both suggest a lower free volume in the sample cured for a longer time (and are consistent with the shrinkage data).

Pursuing the role of the different cure conditions on residual stress in the model epoxy (containing 10 phr 1,4-butanediol), the calculated residual stresses are shown in Table 8. The values represent the average of at least three samples, and the indicated uncertainty represents one standard deviation. There

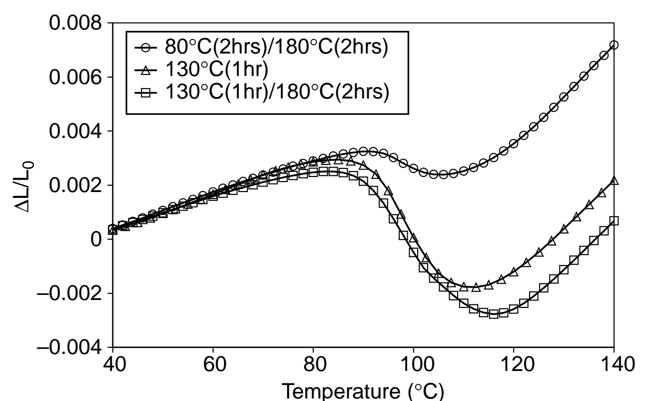

Fig. 15. Dilatometry results for the model epoxy with 10 phr 1,4-butanediol and given different cure profiles.

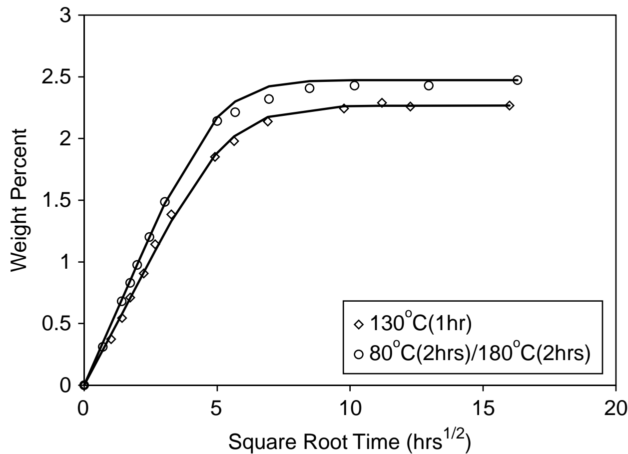

Fig. 16. Weight increase during water immersion at 60 °C for the model epoxy with 10 phr 1,4-butanediol.

Table 8
Influence of cure condition on residual stress

Cure	δ (mm)	σ_r (MPa)
130 °C (1 h)	1.99±0.23	5.49±0.64
80 °C (2 h)/180 °C (2 h)	2.02±0.06	5.54±0.35

is no difference, given the error, in the residual stress generated by the two different curing conditions that we could find. It was expected that the sample with the 80 °C (2 h)/180 °C (2 h) cure would exhibit lower residual stress than the samples cured at 130 °C (1 h) and 180 °C (1 h) based on the above discussion involving shrinkage. However, it is possible that the curvature technique is not sensitive enough to detect changes in residual stress for these very similar networks.

Using the shaft loaded blister test, the adhesion of epoxy to quartz was also measured for the same two cure profiles on the model epoxy containing 10 phr 1,4-butanediol and the results are shown in Fig. 17. After soaking in water at room temperature for 3 days, samples cured at 80 °C (2 h)/180 °C (2 h) exhibited film rupture of the Kapton® backing film (at approximately 130 N) before debonding of the adhesive took place. This indicates that the epoxy/quartz interfacial adhesion was stronger than the Kapton® backing film strength. For the 130 °C (1 h) cure there was no backing film rupture, and it can be seen that crack propagation started to occur at approximately 60 N indicating poorer adhesion than the 80 °C (2 h)/180 °C (2 h) cure. This outcome, however, cannot solely be the consequence of lower stress in that material because samples cured at 130 °C (1 h)/180 °C (2 h) also exhibit high adhesion with rupture of the Kapton® backing film. Therefore, we suggest that it is the higher cure temperatures combined with longer cure times and not the slower initial cure step that increases adhesion. Finally, samples were also tested after soaking in water at 60 °C for 24 h. In this case, the adhesion is lower than that of the samples conditioned at room temperature, and, again, the samples cured with higher temperatures for longer times exhibit better adhesion.

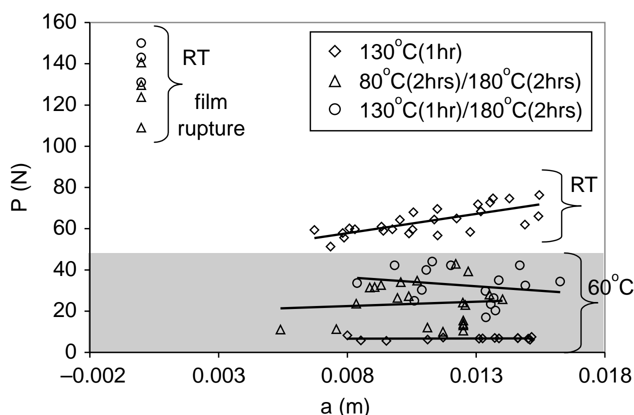

Fig. 17. SLBT results for debonding the model epoxy with different cure profiles from quartz. The specimens were stored in room temperature water for 3 days, or 60 °C water for 1 day. (Note: RT, room temperature).

4. Conclusions

Linear dilatometry revealed that shrinkage occurred in model epoxy samples on heating through the glass transition range. Increasing 1,4-butanediol content in the epoxy led to greater shrinkages detected by the dilatometer arising from an increase the free volume created from the 1,4-butanediol. Consequently, polymer mobility at the glass transition temperature was increased and allowed for greater polymer relaxation and stress relief upon heating. Increasing the 1,4-butanediol content decreased the crosslink density in the epoxy and decreased the residual stress. With increasing 1, 4-butanediol content, the saturation water content increased. Soaking the epoxies in water at 60 °C led to a 17% drop in the modulus, and stress relaxation was also enhanced in the presence of moisture. However, even at higher levels of water sorption, adhesion of the epoxy to quartz was increased by adding the 1,4-butanediol, which can be attributed to greater strain energy dissipation capability.

Advancing the cure at a lower temperature before any postcure reduced the amount of shrinkage observed by the dilatometer. However, within the experimental error, no changes were observed in the measured residual stress for different cure conditions of the epoxy, but overall, higher cure temperatures and longer cure times led to improvements in adhesion.

Acknowledgements

We thank the Hewlett Packard Company, the Adhesive and Sealant Council Education Foundation, and the Center for Adhesive and Sealant Science for providing funding for this project. We also thank the Shell Corporation for donating the epoxy resin.

References

[1] White SR, Hahn HT. J Compos Mater 1993;27:1352–78.
[2] Wang H, Tong-yin Y. Polym Polym Compos 1995;3:369–74.
[3] Naito C, Todd M. Microelectron Reliab 2002;42:119–25.
[4] Crasto AS, Kim RY. J Reinf Plast Comp 200;12:545–58.
[5] Lange J, Toll S, Manson J, Hult A. Polymer 1997;38:809–15.
[6] Ochi M, Yamashita K, Shimbo M. J Appl Polym Sci 1991;43:3013–9.
[7] Brahatheeswarean C, Gupta VB. Polymer 1993;34:289–94.
[8] Voloshin AS, Tsao PhH, Pearson RA. J Electron Packaging 1998;120:314–8.
[9] Chung H, Jang W, Hwang J, Han H. J Polym Sci Poly Phys 2001;39:796–810.
[10] Ree M, Swanson S, Voksen W. Polymer 1993;34:1423–30.
[11] Jou I, Hsu L. J Appl Polym Sci 1992;44:191–8.
[12] Ooi SK, Cook WD, Simon GP, Such CH. Polymer 2000;41:3639–49.
[13] Vogt J. J Adhes 1987;22:139–51.
[14] Timoshenko S. J Opt Soc Am 1925;11:233–55.
[15] Dillard DA, Yu J. In: Mittal KL, editor. Adhesion measurements of films and coatings, vol. 2, 2001. p. 329–40.
[16] Dillard D, Park T, Chen B, Yu J, Guo S, Cao Y, et al. NATAS Notes 2001;32:10–14.
[17] Guo S, Yu J, Willams S, Cao Y, Dillard D. Proceedings of the 24th annual meeting of the adhesion society; 2001. p. 116–8.
[18] Malyshev BM, Salganik RL. Int J Fract Mech 1965;1:114–28.
[19] Wan KT, Mai YW. Int J Fract Mech 1995;74:181–97.
[20] Wan KT, DiPrima A, Ye L, Mai YW. J Mater Sci 1996;31:2109–16.
[21] Wan KT. J Adhes 1999;70:209–19.
[22] Wan KT, Liao K. Thin Solid Films 1999;352:167–72.
[23] Liao K, Wan KT. J Compos Technol Res 2001;23:15–20.
[24] O'Brien EP, Ward TC, Guo S, Dillard DA. J Adhes 2003;79:69–97.
[25] O'Brien EP, Case SL, Ward TC. J Adhes 2005;81:41–58.
[26] Ward IM, Hadley DW. In: An introduction to the mechanical properties of solid polymers. New York, NY: Wiley; 1993 p. 36–40.
[27] Bair HE, Boyle DJ, Ryan JT, Taylor CR, Tighe SC, Crouthamel DL. Polym Eng Sci 1990;30:609–17.
[28] Case SL, Ward TC. J Adhes 2004;80:1079–101.
[29] Shen CH, Springer GS. J Compos Mater 1976;10:2–20.